POTENT UREASE INHIBITORS: DESIGN, SYNTHESIS, MOLECULAR DOCKING AND *IN-SILICO* ADME EVALUATION OF DIHYDROPYRIMIDINE PHTHALIMIDE HYBRIDS

Ahmed A. E. Mourad[1,*], Mai A. E. Mourad[2]

[1] Department of Pharmacology and Toxicology, Faculty of Pharmacy, Port-Said University, Port-Said, Egypt.

[2] Department of Medicinal Chemistry, Faculty of Pharmacy, Port-Said University, Port-Said, Egypt.

*__Corresponding author: Email__: ahmed.mourad@yahoo.com

ABSTRACT

Urease inhibition has gained much attention for management of several gastrointestinal and kidney related diseases including peptic ulcer, urolithiasis as well as pyelonephritis. In the current study, novel dihydropyrimidine phthalimide hybrids were synthesized and evaluated for their *in vitro* urease inhibitory activity. The synthesized hybrids were tested their cytotoxic activity. Additionally, the pharmacokinetic properties and drug-likeness were calculated for all synthesized hybrids. Among the synthesized hybrids, compounds **10g**, **10e**, **10h**, **10i,** and **10j** achieved greater urease inhibitory activity with IC_{50} range of 12.6 ± 0.1 to 20.1 ± 1.3 µM, compared to the standard urease inhibitor, thiourea with IC_{50} of 21.0 ± 0.1 µM. Consistent with our findings, the molecular docking study revealed that the most active compounds are docked well with the active sites of urease enzyme. The structure activity relationship concluded that electronic nature, lipophilicity and steric factor of the substituents markedly influenced the urease inhibitory activity. The pharmacokinetic study showed that our compounds have high oral bioavailability, poor blood brain barrier and CNS permeability as well as they have no teratogenic potential. Finally, the synthesized hybrids are considered safe as indicated by the *in vitro* cytotoxicity assay.

Keywords : Urease inhibitors, Dihydropyrimidine, Phthalimide, Cytotoxicity, Peptic ulcer, Pyelonephritis, *Helicobacter pylori*.

1. Introduction

Urease hydrolyses urea into ammonia and carbamate. At the physiological pH, carbamate in turn spontaneously breaks down into another molecule of ammonia and carbonic acid **(Li et al., 2008)**. Ureases are biosynthesized by a variety of organisms, including plants, fungi and bacteria; and also exist in nature **(Collinand and Orazio, 1993; Krajewska and Ureases, 2009)**. Although urease is the first enzyme to be isolated and crystallized, its behavior inside the body is not fully discovered **(Weber et al., 2008)**. Urease is greatly implicated in pathogenesis of several gastrointestinal diseases including gastric and peptic ulcers **(Hameed et al., 2010; Taha et al., 2015)**. In the same context, Helicobacter pylori is considered as a major causative agent of peptic ulcers **(Hooi et al., 2017)**. Meanwhile, overexpression of urease enzyme leads to interminable formation of ammonia which boosts the ability of *H. pylori* to encounter the acidic environment of the stomach resulting in gastric inflammation, damaging of gastric mucosa permeability **(Stingl et al., 2002)**. Furthermore, this continuous release of ammonia ultimately increased the risk of developing duodenal and peptic ulcers, gastric adenocarcinoma and gastric lymphoma which may eventually cause cancer of the gastric mucosa **(Jr and Blaser, 2002)**.

Moreover, urease is one of the crucial agents that mediate pyelonephritis, urolithiasis, catheter incrustation and hepatic encephalopathy **(Mulvaney and Bremner, 1981, Bayerdörffer and Ottenjann, 1988; Mobley et al., 1995)**. Fortunately, the family of ureases shares common structural moieties, thus targeting one isozyme will affect the other members of ureases **(Macomber et al., 2015)**.

Therefore, the discovery of effective and secure urease inhibitors is emerged as an important target. In the same context, dihydropyrimidinones are known to possess a wide range of biological activities including urease inhibition **(Khan et al., 2016; Muhammad et al., 2017; Iftikhar et al., 2017; Shamim et al., 2018)**, DPP-4 inhibiton **(Mourad et al., 2021),** anti-inflammatory **(Gong et al., 2015)**, antihypertensive **(Putatunda et al., 2014)**, anticancer **(Hameed et al. 2013)** and antimicrobial effects **(Rego et al., 2018)**. Moreover, 3,4-dihydropyrimidin-2(1H)-ones and 4,6-dihydroxypyrimidinediones were reported as potent urease inhibitors (**Muhammad et al., 2017; Shamim et al., 2018)** Additionally, benzylidene indane-1,3-diones and its derivatives have been reported for their potential urease inhibitory activity **(Bano et al., 2018)** (Figure 1).

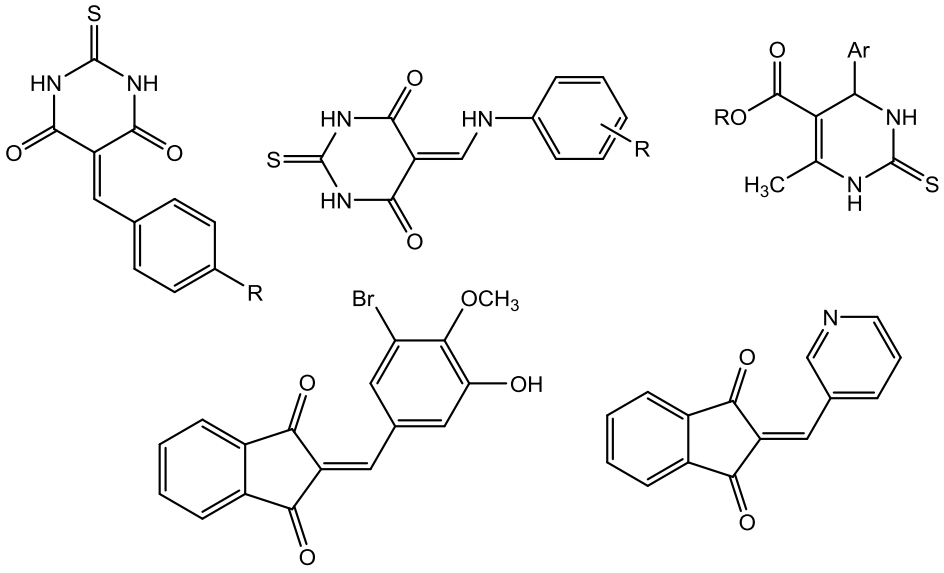

Figure 1. Reported dihydropyrimidinediones and benzylidene indane-1,3-diones based urease inhibitors.

So, in the view of the therapeutic importance of urease inhibition, we herein, aimed at utilizing drug design strategy to develop novel entities from gathering dihydropyrimidine and phthalimide moieties; and evaluating their urease inhibitory activity and their safety profile (Figure 2, Scheme 1). Furthermore, the molecular docking study of the synthesized hybrids was performed to get insight into the binding pattern within the protein active site; as well as the pharmacokinetic parameters and the drug-likeness of the synthesized hybrids were further evaluated.

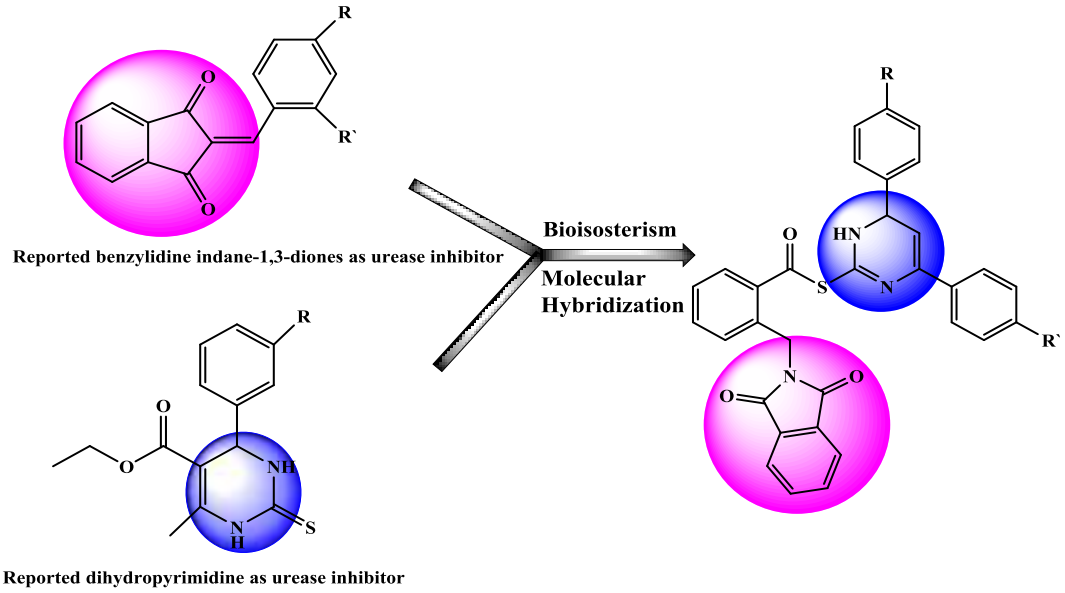

Figure 2. Diagram represents design of novel urease inhibitors

2. Materials and methods

2.1. Urease inhibition assay

In 96 well plates, 25 µl of Jack bean (*Canavalia ensiformis*) urease, 55 µl of 100 mM urea and various concentrations of synthesized compounds were incubated for 15 min at 30ºC. Different concentrations of both synthesized hybrids and substrate were used. Phenol reagent (0.005% w/v of sodium nitroprusside with 1% w/v phenol) and alkali reagent (0.5% of w/v NaOH with 0.1% of w/v NaOCl) were added to each well. Indophenols method was adopted to evaluate the urease activity based on production of ammonia as previously described (**Weatherburn, 1967**). Fifty min later, the alteration in absorbance at 630 nm was assessed using microplate absorbance reader (Bio-Rad Laboratories, Hercules, CA, USA). All reactions were done in triplicate up to a final volume of 200 µl. Thiourea was used as a reference urease inhibitor.

2.2. Cytotoxicity assay

Murine 3T3-L1 cells were seeded at a density of 2.5×10^4 cells per well into 96-well plates until confluent in Dulbecco's modified Eagle's medium (DMEM) containing low glucose (1000 mg/L), 10% Fetal bovine serum (FBS), penicillin (100 units/mL) and streptomycin (100 µg/mL). The cells were incubated in a humidified atmosphere containing 5% CO_2 in air at 37°C. Two days post-confluent, differentiation was induced by replacing the medium with differentiation medium [DMEM (high glucose: 4500 mg/L) supplemented with 10% FBS, 1 µM dexamethasone, 0.5 mM IBMX, and 5 µg/mL insulin]. Three days later, the differentiation medium was replaced with a maintenance medium [DMEM (high glucose) supplemented with 10% FBS and 5 µg/mL insulin]. After 2 days (on day 6), the medium was replaced by fresh medium, and the cells were cultured for a further 2 days.

On day 8 (post confluent), serial dilutions of our synthesized hybrids (12.5-100 µg/ml) were added to each well. Two days later, MTT reagent was added and the plates were incubated in a CO_2 incubator at 37°C for 2 h. The amount of formazan dye was measured spectrophotometrically at 590 nm using microplate absorbance reader (Bio-Rad Laboratories, Hercules, CA, USA) (**Mourad et al., 2020).**

2.3. Molecular docking

Molecular docking study of the synthesized hybrids (**10a-j**) as well as the reference compound, thiourea, were performed using MOE software. Ligands were built into the builder interface of the MOE program and their energies were minimized until a RMSD (root mean square deviations) gradient of 0.01 kcal/mol and RMS (Root Mean Square) distance of 0.1 Å with MMFF94× (Merck molecular force field 94×) force-field and the partial charges were automatically calculated. The X-ray crystallographic structure of urease protein (PDB code: 4UBP, resolution 2.25 Å), was downloaded from protein data bank (www.rcsb.org). The enzyme was prepared, the hydrogens were added as well as the atoms connection and type were checked with automatic correction.

The obtained poses were studied and the poses which showed the best ligand-enzyme interactions were selected and stored for energy calculations.

2.4. Pharmacokinetic properties prediction

Pharmacokinetic properties as well as the drug-like nature of the synthesized hybrids (**10a-j**) were calculated and predicted based on online pkCSM software via the link, http://biosig.unimelb.edu.au/pkcsm/prediction .

2.5. Statistical analysis

Results were expressed as means ± standard error of the mean (SEM) and were analyzed using GraphPad Prism® (GraphPad Software, San Diego California USA).

3. Chemistry

The target hybrids (**10a-j**) in Scheme 1 were synthesized in our laboratories and experienced significant DPP-4 inhibitory activity. The full details of their synthesis, spectroscopic as well as the elemental characterization can be found in our recent previous publication **(Mourad et al., 2021)**.

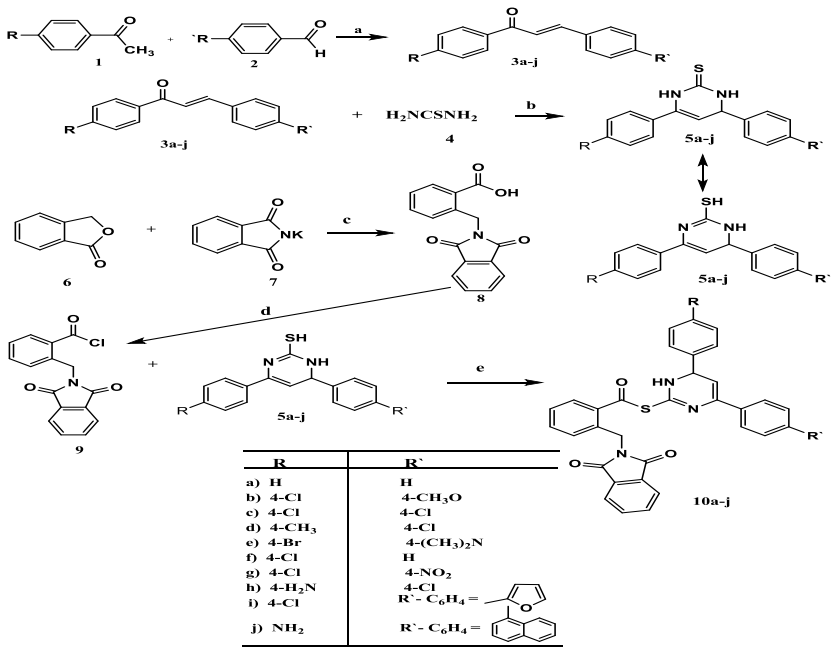

Scheme 1. Synthesis of the target compounds 10a-j
Reagents and conditions: a)NaOH, dil. EtOH, r. t. ; b)NaOH, abs. EtOH; c)DMF, reflux; d)$SOCl_2$, reflux, dry benzene, distillation; e) abs. dichloromethane, TEA, r.t.

4. Results

4.1. *In vitro* urease inhibition

The synthesized hybrids (**10a-j**) were evaluated for their *in vitro* urease inhibitory activity. Table 1 and Figure 3 showed that **10g**, **10e**, **10h**, **10i** and **10j** hybrids exhibited potent urease inhibition with IC_{50} values of 12.6 ± 0.1, 15.2 ± 0.7, 15.8 ± 0.5,

17.4 ± 1.1 and 20.1 ± 1.3 µM, respectively, much better than thiourea, the reference urease inhibitor with IC_{50} value of 21.0 ± 0.1 µM. Compared to thiourea, **10b** hybrid showed slightly lower urease inhibitory activity with IC_{50} value of 28.2 ± 2.1 µM. Moreover, **10f** and **10d** hybrids almost had similar urease inhibitory activity with IC_{50} values of 37.5 ± 2.6 and 38.7 ± 1.9 µM, respectively. Among the synthesized hybrids, **10c** and **10a** hybrids showed the weakest urease inhibitory activity with IC_{50} values of 44.3 ± 0.8 and 56.4 ± 2.2 µM, respectively.

Table 1: Urease inhibitory activity (IC_{50}) of (**10a-j**) hybrids and thiourea.

Compound No.	IC_{50} ±SEM (µM)
10a	56.4 ± 2.2
10b	28.2 ± 2.1
10c	44.3 ± 0.8
10d	38.7 ± 1.9
10e	15.2 ± 0.7
10f	37.5 ± 2.6
10g	12.6 ± 0.1
10h	15.8 ± 0.5
10i	17.4 ± 1.1
10j	20.1 ± 1.3
Thiourea	21.0 ± 0.1

Data were expressed as mean ± standard error of mean (SEM) of three independent experiments.

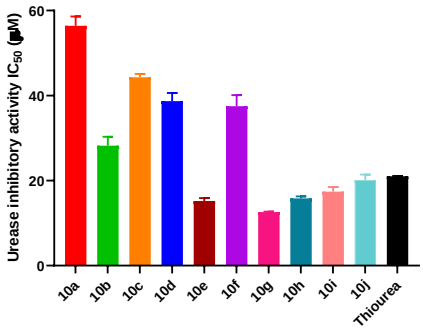

Figure 3: Urease inhibitory activity (IC_{50}) of (**10a-j**) hybrids and thiourea

Data were expressed as mean ± standard error of mean (SEM) of three independent experiments.

4.2. Cytotoxicity assay

The cytotoxicity of the synthesized hybrids (**10a-j**) was evaluated in 3T3-L1 cells. Fortunately, all compounds showed non-toxic behavior as evident by their high IC_{50} values that ranged from 19.6 ± 1.5 to 55.3 ± 1.8 µM compared to the standard cyclohexamide with IC_{50} value of 0.46 ± 0.2 µM (Table 2 and Figure 4).

Table 2: Cytotoxicity assay of (**10a-j**) hybrids and Cyclohexamide.

Compound No.	IC_{50} ±SEM (µM)
10a	34.6 ± 2.1
10b	41.1 ± 2.7
10c	55.3 ± 1.8
10d	19.6 ± 1.5
10e	52.7 ± 3.4
10f	36.9 ± 1.1
10g	50.2 ± 2.8
10h	47.8 ± 3.1
10i	51.5 ± 1.7
10j	27.8 ± 2.3
Cyclohexamide	0.46 ± 0.2

Data were expressed as mean ± standard error of mean (SEM) of three independent experiments.

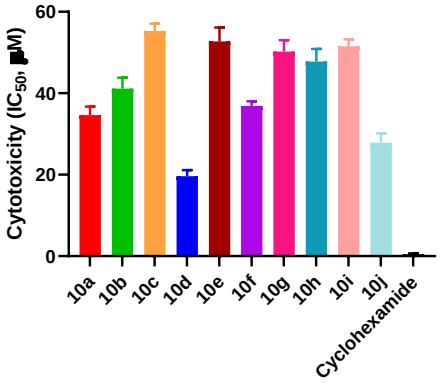

Figure 4: Cytotoxicity assay of (**10a-j**) hybrids and Cyclohexamide.

Data were expressed as mean ± standard error of mean (SEM) of three independent experiments.

4.3. Molecular docking study

Docking at urease active site

In order to explore the possible binding modes of the synthesized hybrids (**10 a-j**) with their respective target protein, molecular docking study was carried out using MOE program where the 3D structure of the urease active sites is available at RCSB Protein Data Bank, [PDB code: 4UBP, resolution 2.25 Å (www.rcsb.org)]. Thiourea was used as a reference compound. Table 3**,** showed the energy binding scores and binding interactions of the titled hybrids (**10a-j**). Importantly, the results cleared that nearly most of the synthesized hybrids were successfully docked into urease protein

and achieved energy binding scores higher than thiourea. Moreover, they had significant binding interactions with the urease active sites such as, Ala 366, Ala 170, Asp 363, Cys 322, His 222, His 275 and Ni ion which explained their potential urease inhibitory activity **(Ansari et al., 2009)**.

Notably, **10g** hybrid possessed the highest binding energy score and the highest urease inhibitory activity where it has similar interaction pattern to the reference compound and consequently good fitting with the receptor active sites. However, **10g** hybrid is engaged in network interactions with Ni 798 of protein and formed strong hydrogen bonding interactions with Ala 170, Cys 322 and His 222 residues. Additionally, Ni 798 and Ni 799 are further coordinated by His 249, His 275, KCX 220, Asp 363, His 137 and His 139 residues, as shown in (Figure 5 C&D).

Similarly, **10e** hybrid formed strong hydrogen bonding interactions with the key amino acids residues in the binding sites which positively affected its *in vitro* urease inhibitory activity. The bromine atom, sulphur atom and the free NH group in the dihydropyrimidine ring of this compound interact by three hydrogen bonds with Ala 366 and His 275. As well as, Ni 798 and Ni 799 bonded with KCX 220, His 249, His 275, His 137, His 139 and Asp 363 (Figure 5 A&B).

Of considerable interest, the binding mode showed that the sulphur atom, nitrogen atom, free NH, carbonyl oxygen and the methylene group of **10h** hybrid participated by six hydrogen bonding network with Ala 366, Cys 322, Lys 169, Leu 365 and Gly 280 residues. Additionally, Ni 798 and Ni 799 further bonded with KCX 220, His 249, His 275, His 137, His 139 and Asp 363 (Figure 5 E&F). On the other hand, Ala 366 residue formed strong hydrogen bond with sulphur atom of **10i** hybrid in addition to another π-cation bond with Lys 169.

However, the IC_{50} values of **10b** and **10d** hybrids were less than that of thiourea which may be attributed to the formation of weak π-hydrogen bonding interactions with the key amino acid Ala 170, beside another hydrogen bonds and π-cation bonding interaction with Asp 224 and Lys 169 residues. Notably, the electron withdrawing effect of chlorine atom negatively affected the IC_{50} values of **10c** and **10f** hybrids which could be explained by the formation of weak π-hydrogen bonding interactions between the phenyl rings of these compounds and Ala 170, Asp 224, Glu 166, Lys 169 and His 323 residues. Additionally, another hydrogen bond formed between the chlorine atom of **10c** hybrid and Gly 280 residue.

In the same context, the unsubstituted **10a** hybrid lost its urease inhibitory activity owing to the formation of only one weak π-hydrogen bonding interaction with Ala 170 residue. Finally, it can be concluded that most of the synthesized hybrids are able to interact with the crucial amino acids in the urease protein and thus are able to inhibit its activity efficiently.

Table 3: Types of binding interactions and energy scores (kcal/mol) for (**10a-j**) hybrids and thiourea at the urease active site.

Compound No.	Types pf Interactions	Energy Scores
10a	- One π-hydrogen bonding interaction with Ala 170 (4.11 Å).	-5.90
10b	- One hydrogen bonding interaction with Asp 224 (2.99 Å). - Two π-hydrogen bonding interaction with Ala 170 and Asp 224 (4.20 and 3.99 Å).	-6.69
10c	- One hydrogen bonding interaction with Gly 280 (3.85 Å). - Two π-hydrogen bonding interaction with Ala 170 and Asp 224 (3.81 and 4.41 Å). - One π-cation bonding interaction with Lys 169 (4.11 Å). -Ni 798 bonded to KCX 220, His 249 and His 275 (1.95, 1.96 and 2.03 Å).	-6.46
10d	-Two π-hydrogen bonding interaction with Ala 170 and Asp 224 (3.80 and 4.22 Å). - One π-cation bonding interaction with Lys 169 (4.27 Å). - Ni bonded to KCX 220, His 249 and His 275 (1.95, 1.96 and 2.03 Å).	-6.47
10e	- Two hydrogen bonding interaction with Ala 366 (3.49 and 2.98 Å). - One hydrogen bonding interaction with His 275 (3.32 Å). - Ni 798 bonded with KCX 220, His 249 and His 275 (1.95, 1.96 and 2.03 Å). - Ni 799 bonded with His 137, His 139, Asp 363 and KCX 220 (1.99, 1.99, 2.04 and 2.07 Å). - Ni 799 bonded with two ionic bonds with Asp 363 and His 137 (2.07 and 1.99 Å).	-6.45
10f	- Three π-hydrogen bonding interaction with Glu 166, Lys 169 and His 323 (4.08, 4.27 and 3.59 Å).	-6.63
10g	-One metallic interaction with Ni 798 (2.84 Å). - Two hydrogen bonding interaction with Cys 322 and His 222 (3.26, 3.36 Å). - Ni 798 bonded with KCX 220, His 249 and His 275 (1.95, 1.96 and 2.03 Å). - One π-hydrogen bonding interaction with Ala 170 (4.11 Å). - Ni 799 bonded with metallic bonds with His 137, His 139, KCX 220 and Asp 363 (1.99, 1.99, 2.04 and 2.07 Å). - Ni 799 bonded with two ionic bonds with Asp 363 and His 137 (2.07 and 1.99 Å).	-7.29
10h	- Six hydrogen bonding interaction with Ala 366, Cys 322, Lys 169, Leu 365 and Gly 280 (2.91, 3.98, 3.44, 3.24, 3.93 and 2.85Å). - Ni 798 bonded with metallic bonds with KCX 220, His 249 and His 275 (1.95, 1.96 and 2.03 Å) - Ni 799 bonded with metallic and ionic bonds with KCX 220, Asp 363, His 137 and His 139 (2.04, 2.07, 1.99 and 2.07 Å)	-6.52
10i	- One hydrogen bonding interaction with Ala 366 (3.24 Å). - One π-cation bonding interaction with Lys 169 (4.01 Å).	-6.45
10j	- One hydrogen bonding interaction with Asp 332 (3.62 Å). - Two π-hydrogen bonding interaction with Ala 170 (4.05 and 4.15 Å).	-6.39
Thiourea	- Two hydrogen bonding interaction with Ala 170 and His 222 (3.05 and 3.80 Å). - Two metallic interaction with Ni 798 and Ni 799 (2.33 and 2.80 Å).	-5.02

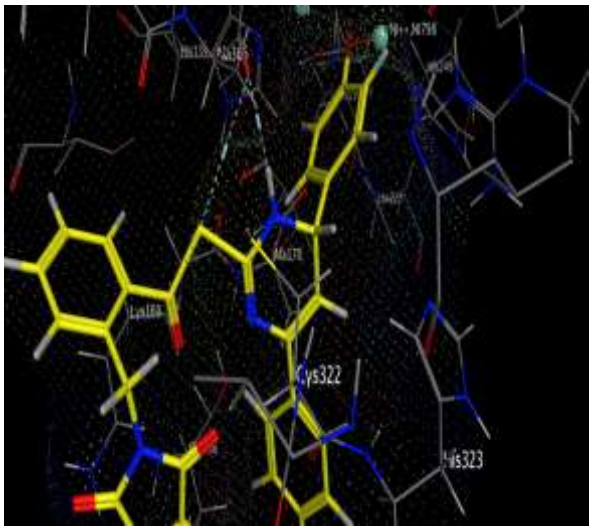

A

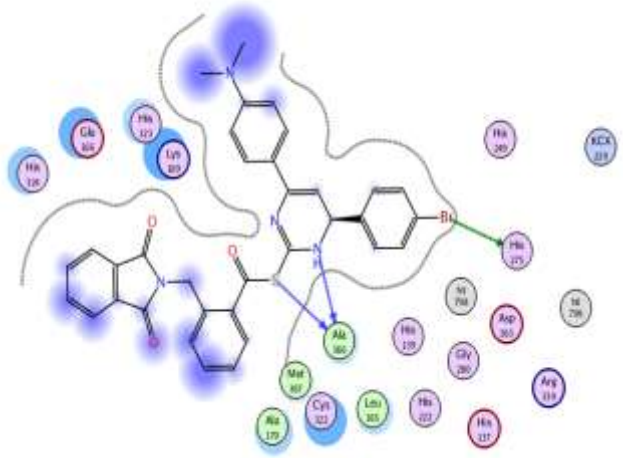

B

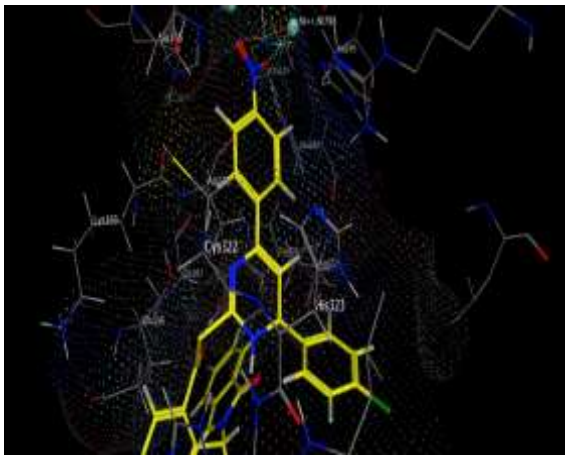

C

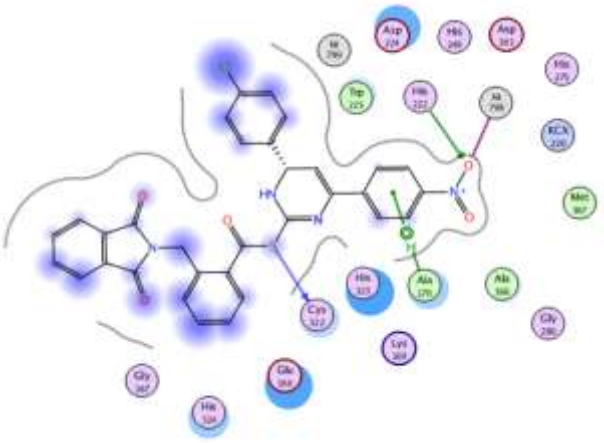

D

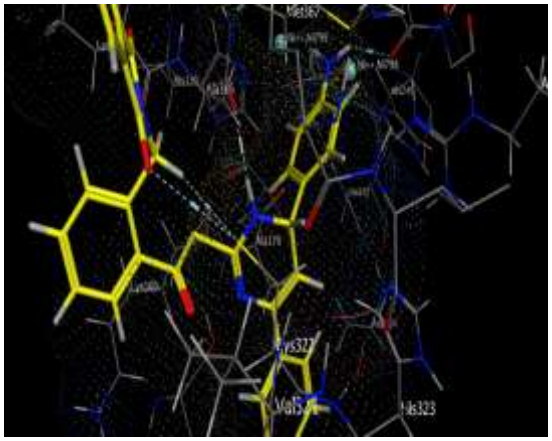

E

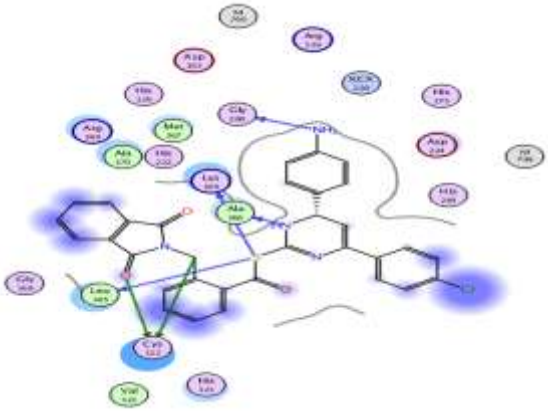

F

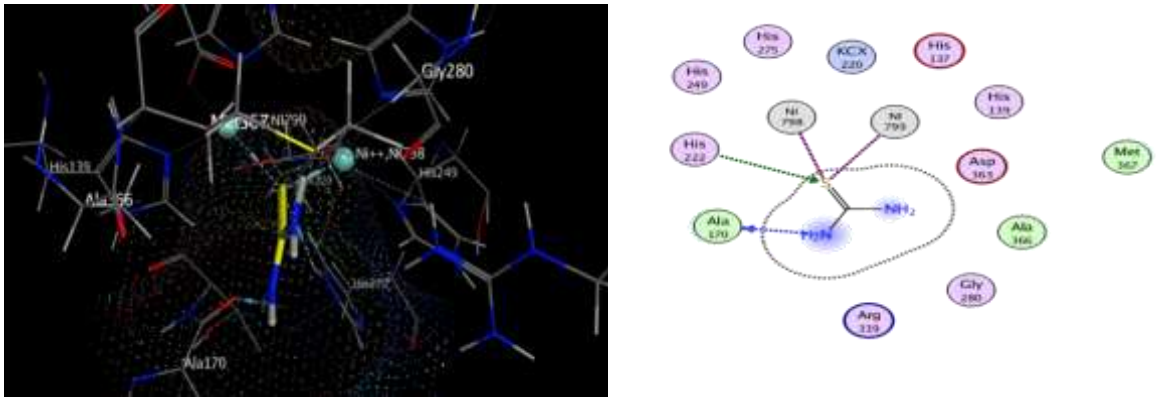

G **H**

Figure 5. Docking and binding pattern of compounds **10e**, **10g, 10h** and thiourea showing interactions with different amino acid residues found in the urease active site (PDB code: 4UBP).

(A) 3D structure of compound **10e** (yellow) (B) 2D structure of compound **10e**.

(C) 3D structure of compound **10g** (yellow) (D) 2D structure of compound **10g**.

(E) 3D structure of compound **10h** (yellow) (F) 2D structure of compound **10h**. (G) 3D structure of thiourea (yellow) (H) 2D structure of thiourea.

4.4. *In silico* ADMET prediction

Pharmacokinetics are complex processes that constitute the effect of the body on the administrated drug. Pharmacokinetics start by absorption and distribution steps and end by process of disposition that involves metabolism and excretion. The pharmacokinetic profile of the synthesized hybrids (**10a-j**) was predicted using pkCSM pharmacokinetic prediction program.

4.4.1. Absorption studies

Several pharmacokinetic parameters that could affect absorption rate were evaluated for the synthesized hybrids. Among the calculated parameters, water solubility, human intestinal absorption (HIA), Caco-2 cell permeability, being a P-glycoprotein substrate or I/II inhibitor.

According to the results presented in Table 4**,** synthesized hybrids (**10a-j**) had moderate water solubility that positively reflected on distribution. Additionally, Caco-2 permeability results predicted significant *in vivo* absorption rate via small intestine. Consequently, the synthesized compounds exhibited high HIA values that ranged from 86.56% to 100% which indicated that the synthesized hybrids have good oral bioavailability. Furthermore, (**10a-j**) hybrids act as P-glycoprotein substrate as well as P-glycoprotein I/II inhibitors.

Table 4: Absorption properties of the synthesized hybrids (**10a-j**).

Property	10a	10b	10c	10d	10e	10f	10g	10h	10i	10j
Water solubility	- 4.97	-4.84	- 4.89	- 4.95	-4.72	-4.99	-4.47	- 4.06	-4.74	-3.94
Caco2 permeability	0.43	0.54	0.47	0.52	0.55	0.45	0.22	0.59	0.76	0.43
Human intestinal absorption (%absorbed)	89.38	89.03	86.56	88.01	89.29	87.98	100	97.87	100	100
Skin permeability	-2.73	-2.73	- 2.73	- 2.73	-2.73	-2.73	-2.73	-2.74	-2.74	-2.74
P-glycoprotein substrate	Yes	Yes	yes	Yes	Yes	Yes	Yes	Yes	Yes	Yes
P-glycoprotein I inhibitor	Yes	Yes	Yes	Yes	Yes	Yes	Yes	Yes	Yes	Yes
P-glycoprotein II inhibitor	Yes	Yes	Yes	Yes	Yes	Yes	Yes	Yes	Yes	Yes

4.4.2. Distribution studies

Parameters that affect distribution of our synthesized hybrids (**10a-j**) including volume of distribution V_d, blood brain barrier penetration (BBB) and plasma protein binding (PPB) were calculated. As shown in Table 5, all the synthesized hybrids have acceptable V_d , poor BBB and CNS permeability.

Table 5: Distribution properties of the synthesized hybrids (**10a-j**).

Property	10a	10b	10c	10d	10e	10f	10g	10h	10i	10j
VDss (human)	-0.51	-0.46	- 0.39	-0.39	-0.32	-0.45	-0.75	-0.57	-0.11	-1.16
Fraction unbound (human)	0	0	0	0	0	0	0.007	0.005	0	0.103
BBB permeability	-0.002	-0.38	-0.34	-0.17	-0.29	-0.17	-0.64	-0.92	-0.38	-0.92
CNS permeability	-1.39	-1.47	-1.16	-1.20	-1.35	-1.27	-1.51	-1.42	-1.42	-1.33

4.4.3. Metabolism and excretion studies:

With regard to liver microsomal enzymes, the calculated data showed that almost all hybrids (**10a-i**) are neither substrate nor inhibitor of CYP2D6. On contrary, all synthesized hybrids (**10a-i**) are CYP3A4 substrates and inhibitors (except **10j**). Similarly, all synthesized hybrids were found to be CYP2C19 inhibitors. Meanwhile, **10a**, **10f** and **10h-10j** hybrids were considered as CYP1A2 inhibitors. Regarding CYP2C9, **10a**, **10b**, **10h** and **10i** hybrids were classified as inhibitors.

Finally, the synthesized hybrids (**10a-j**) exhibited an acceptable clearance rate (Table 6).

Table 6: Metabolism and excretion properties of the synthesized hybrids (**10a-i**).

Property	10a	10b	10c	10d	10e	10f	10g	10h	10i	10j
CYP2D6 substrate	No	No	No	No	No	No	No	No	No	Yes
CYP3A4 substrate	Yes	Yes	Yes	Yes	Yes	Yes	Yes	Yes	Yes	Yes
CYP1A2 inhibitor	Yes	No	No	No	No	Yes	No	Yes	Yes	Yes
CYP2C19 inhibitor	Yes	Yes	Yes	Yes	Yes	Yes	Yes	Yes	Yes	Yes
CYP2C9 inhibitor	Yes	Yes	No	No	No	No	No	Yes	Yes	No
CYP2D6 inhibitor	No	No	No	No	No	No	No	No	No	No
CYP3A4 inhibitor	Yes	Yes	Yes	Yes	Yes	Yes	Yes	Yes	Yes	No
Total Clearance	0.02	-0.13	-0.19	- 0.11	-0.09	-0.11	-1.51	-0.28	-0.06	-0.19
Renal OCT2 substrate	No	No	No	No	No	No	No	No	No	No

4.4.4. Toxicity studies

AMES test is used to predict the mutagenic potential of the investigated compounds. Fortunately, all synthesized hybrids lack mutagenic potential, as shown in Table 7.

Table 7: Toxicity properties of the synthesized hybrids (**10a-i**).

Property	10a	10b	10c	10d	10e	10f	10g	10h	10i	10j
AMES toxicity	No	No	No	No	No	No	No	No	No	No
Max. tolerated dose (human) (log mg/kg/day)	0.08	-0.10	-0.01	-0.01	-0.02	0.03	-0.07	0.15	-0.06	0.30
hERG I inhibitor	No	No	No	No	No	No	No	No	No	No
hERG II inhibitor	Yes	Yes	Yes	Yes	Yes	Yes	Yes	Yes	Yes	Yes
Oral Rat Acute Toxicity (LD50) (mol/kg)	2.59	2.54	2.58	2.59	2.59	2.58	2.92	2.14	2.54	2.54
Oral Rat Chronic Toxicity(LOAEL)(logmg/kg/day)	2.16	1.99	2.03	1.99	1.96	2.10	2.67	2.09	1.49	3.54
Hepatotoxicity	Yes	Yes	Yes	No	No	Yes	Yes	Yes	No	Yes
Skin Sensitization	No	No	No	No	No	No	No	No	No	No

4.4.5. Drug-likeness Characters

Scores of drug-likeness of all synthesized hybrids (**10a-j**) are presented in Table 8. Notably, compound with zero or negative score is lacking drug –likeness. Interestingly, **10b**, **10d**, **10h**, **10c**, **10f** and **10i** hybrids have the highest drug-likeness scores that ranged from 1.07 to 0.87. On the other hand, **10a** hybrid had the lowest drug-likeness score (0.25).

Finally, it can be concluded that the synthesized hybrids are likely to be orally active, having good intestinal absorption, having poor BBB and CNS permeability, lacking mutagenic potential as well as they possessed promising drug likeness characteristics.

Table 8: Prediction of drug-likeness model score of the synthesized hybrids (**10a-i**).

Compound no.	Drug-likeness model score by MolSoft
10a	0.25
10b	1.07
10c	0.89
10d	0.95
10e	0.58
10f	0.89
10g	0.65
10h	0.95
10i	0.87
10j	0.53

5. Discussion

The present study aimed at synthesizing dihydropyrimidine phthalimide hybrids and evaluating their *in vitro* urease inhibitory activity. We focused our design on molecular modification of substituents in the *para*-position of aromatic rings in positions 4 and 6 of 1,6-dihydropyrimidines moiety as well as the size and type of this substituents. The results showed in Table 1 indicated that **10g** hybrid exhibited the most potent urease inhibitory activity among the other synthesized hybrids with IC_{50} value of (12.6 ± 0.1 µM), much better than thiourea, the reference urease inhibitor, with IC_{50} value of (21.0 ± 0.1 µM). This behavior may be attributed to the ionic character of the *p*-nitro group that markedly enhances its binding pattern with nickel ion and with the key amino acids present in the receptor active site.

Moreover, compounds **10e** and **10h** possessed nearly equal urease inhibitory activity to that of **10g** hybrid; as indicated by their IC_{50} values 15.2 ± 0.7, 15.8 ± 0.5 µM, respectively. Interestingly, despite the large size of both *p*-bromophenyl and *p*-dimethylaminophenyl groups in **10e** hybrid, the electronegativity of the substituents played the major role in enhancing its binding mode with the active receptor site which consequently improved its urease inhibitory activity.

Additionally, the potent urease inhibitory activity of **10h** hybrid may be owed to the presence of lone pair of electrons on the nitrogen atom which make it successfully

able to form strong hydrogen bond network with the crucial amino acids in the active site. Furthermore, IC_{50} values of **10i** and **10j** hybrids were (17.4 ± 1.1 and 20.1 ± 0.1 µM), respectively, less than that of thioureae. The urease inhibitory activity of **10i** hybrid backed to the small size of furanyl group which makes it more suitable for the fitting to the receptor active site. Also, the nitrogen lone pair of electrons of **10j** hybrid enhances its binding to the receptor active sites and consequently supported the urease inhibitory activity.

However, the presence of lipophilic electron donating *p*-methoxyphenyl group positively reflected on urease inhibitory activity of **10b** hybrid that has IC_{50} value slightly larger than IC_{50} value of thiourea. On the other hand, **10c** and **10f** hybrids exhibited weak binding interaction with the key amino acid residue in the receptor site that was evidenced by their high IC_{50} values (44.3 ± 0.8 and 37.5 ± 2.6 µM), respectively. Finally, the unsubstituted **10a** hybrid experienced the lowest urease inhibitory activity (IC_{50}= 56.4 ± 2.2 µM) which was also confirmed by its weak binding interaction with the receptor active site. Accordingly, it can be concluded that the nature of the substituents, lipophilicity, electronic nature as well as the steric factor greatly influenced the biological activity of the system incorporated.

Of considerable interest, the cytotoxicity results indicated that the synthesized hybrids (**10a-j**) were considered safe compared to the reference compound. Moreover, the molecular docking study showed that most of the synthesized hybrids bind efficiently to the key amino acids in the active receptor site which positively reflected on their urease inhibitory activity. In the same context, the performed pharmacokinetic study revealed that the synthesized hybrids have acceptable pharmacokinetic profile involving good oral bioavailability, distribution, intestinal absorption, no BBB permeability, no mutagenic potential and acceptable clearance rate. Finally, the synthesized hybrids have promising drug-likeness properties.

6. Conclusion

Novel series of dihydropyrimidine phthalimide (**10a-j**) has been synthesized and examined for their urease inhibitory activity. The results indicated that five hybrids **10g**, **10e**, **10h**, **10i** and **10j** exhibited superior urease inhibitory activity with IC_{50} range of 12.6 ± 0.1 to 20.1 ± 1.3 µM, compared to thiourea with IC_{50} of 21.0 ± 0.1 µM. Other synthesized hybrids showed moderate activity. The molecular docking study further supported our findings, with the most active compounds being fitted well with the crucial amino acids in the urease active sites. The structure activity relationship revealed that the nitro, amino and dimethylamino groups are favorable for the inhibitory activity. The pharmacokinetic study showed that most synthesized hybrids have high intestinal absorption, poor CNS permeability, no mutagenicity; as well as they achieved high scores in drug-likeness analysis. According to *in vitro* cytotoxicity assay, the synthesized hybrids considered safe. The novel synthesized urease inhibitors hybrids represent a promising safe and effective candidates that could provide a therapeutic add in the field of urease related pathologies.

REFERENCES

Ansari, F.L., Wadood, A., Ullah, A., Iftikhar, F., Ul-Haq, Z., (2009). In silico studies of urease inhibitors to explore ligand-enzyme interations. J. Enzyme Inhib. Med. Chem. 24, 151–156. https://doi.org/10.1080/14756360801945598.

Bano, B., Khalid, K., Khan, M., Begum, F., Lodhib, M.A., Salara, U., Khalil, R., Ul-Haq, Z., Perveend, S., (2018). Benzylidine indane-1,3-diones: As novel urease inhibitors; synthesis, in vitro, and in silico studies. Bioorg. Chem. 81, 658–671. https://doi.org/10.1016/j.bioorg.2018.09.030.

Bayerdörffer, E., Ottenjann, R., (2009). The role of antibiotics in Scand. J. associated peptic ulcer disease. Gastroenterol. 23, 93–100. https://doi.org/10.3109/00365528809091721.

Collinand, C.M., Orazio, S.E.F.D., (1993). Bacterial ureases: structure, regulation of expression and role in pathogenesis. Mol. Micro. 9, 907–913. https://doi. 10.1111/j.1365-2958.1993.tb01220.x.

Gong, K., Wang, H., Wang, S., Ren, X., (2015). β-Cyclodextrin-propyl sulfonic acid: a new and eco-friendly catalyst for one-pot multi-component synthesis of 3,4-dihydropyrimidones via Biginelli reaction. Tetrahedron. 71, 4830–4834. https://doi.org/10.1016/j.tet.2015.05.028.

Hameed, A., Anwar, A., Khan, K.M., Malik, R., Shahab, F., Siddiq, S., Basha, F.Z., Choudhary, M.I., (2013). Urease inhibition and anticancer activity of novel polyfunctional 5,6-dihydropyridine derivatives and their structure-activity relationship. Eur. J. Chem. 4, 49–52. https://doi.org/10.5155/eurjchem.4.1.49-52.701.

Hameed, A., Khan, K.M., Zehra, S.T., Ahmed, R., Shafiq, Z., Bakht, S.M., Yaqub, M., Hussain, M., Leon, A.D.L.V.D., Bajorath, F.N.J., Ahmad, H., Tahir, M.N., Choudhary, M.I., (2010). Synthesis, Biological evaluation and molecular docking of N-Phenylthiosemicarbazones as urease inhibitors, J. ACS. Med. Chem. Lett. 1, 145–149. https://doi.10.1016/j.bioorg.2015.06.004.

Hooi, J.K.Y., Lai, W.Y., Ng, W.K., Suen, M.M.Y., Underwood, F.E., Tanyingoh, D., Malfertheiner, P., Graham, D.Y., Wong, V.W.S., Wu, J.C.Y., Chan, F.K.L., Sung, J.J.Y., Kaplan, G.G., Ng, S.C., (2017). Global Prevalence of Helicobacter pylori Infection: Systematic Review and Meta-Analysis. Gastroenterol. 153, 420-429.https://doi.10.1053/j.gastro.2017.04.022.

Iftikhar, F., Ali, Y., Kiani, F.A., Hassan, S.F., Fatima, T., Khan, A., Niaz, B., Hassan, A., Ansari, F.L., Rashid, U., (2017). Design, synthesis, in vitro Evaluation and docking studies on dihydropyrimidine-based urease inhibitors. Bioorg. Chem. 74, 53–65. http://dx.doi.org/10.1016/j.bioorg.2017.07.003.

Jr, R.M.P.; Blaser, M.J., (2002). Helicobacter pylori and gastrointestinal tract adenocarcinomas. Nat. Rev. Cancer 2, 28–37. https:// 10.1038/nrc703.

Khan, A., Hashim, J., Arshad, N., Khan, I., Siddiqui, N., Wadood, A., Ali, M., Arshad, F., Khan, K.M., Choudhary, M.I., (2016). Dihydropyrimidine based hydrazine dihydrochloride derivatives as potent urease inhibitors. Bioorg. Chem. 64, 85–96. https://doi.10.1016/j.bioorg.2015.12.007.

Krajewska, B., Ureases, I., (2009). Functional catalytic and kinetic properties: a review, J. Mol. Cat. B: Enzym. 59, 9–21. https://doi.org/10.1016/j.molcatb.2009.01.003.

Li, M., Ding, W., Baruah, B., Cransand, D.C., Wang, R., (2008). Inhibition of protein tyrosine phosphatase 1B and alkaline phosphatase by *bis* (maltolato) oxovanadium (IV). J. Inorg. Biochem. 102, 1846–1853. doi: https://doi.10.1016/j.jinorgbio.2008.06.007.

Macomber, L., Minkara, M.S., Hausinger, M.R.P., Merz, K.M., (2015). Reduction of Urease Activity by Interaction with flap covering the active site. J. Chem. Inf. Model. 55, 354–361. https://doi.10.1021/ci500562t.

Mobley, H.L., Island, M.D., Hausinger, R.P., (1995). Molecular biology of microbial ureases. Microbiol. Rev. 59, 451–480. PMID: 7565414.

Mourad, A.A.E., Khodir, A.E., Saber, S., Mourad, M.A.E., (2021). Novel Potent and Selective DPP-4 Inhibitors: Design,Synthesis and Molecular Docking Study of Dihydropyrimidine Phthalimide Hybrids. Pharmaceuticals. 14, 144-168. https://doi.org/10.3390/ph14020144.

Mourad, A.A.E., Mourad, M.A.E., (2020). Enhancing insulin sensitivity by dual PPARγ partial agonist, β-catenin inhibitor: Design, synthesis of new αphthalimido-o-toluoyl2-aminothiazole hybrids. Life Sciences. 259, 118270-118285. https://doi.org/10.1016/j.lfs.2020.118270.

Muhammad, M.T., Khan, K.M., Arshia, Khan, A., Arshad, F., Fatima, Bibi, Choudhary, M.I., Syed, N., Moin, S.T., (2017). Syntheses of 4,6-dihydroxypyrimidinediones, their urease inhibition, in vitro, in silico, and kinetic studies. Bioorg. Chem. 75, 317–331. https://doi.org/10.1016/j.bioorg.2017.08.018.

Mulvaney, R.L., Bremner, J.M., (1981). Use of urease and nitrification inhibitors for control of urea transformations in soils, in: E.A. Paul, J.N. Ladd (Eds.), Soil Biochem. 5, 153–196.

Putatunda, S., Chakraborty, A., (2014). A Cs_2CO_3-mediated simple and selective method for the alkylation and acylation of 3,4-dihydropyrimidin-2(1*H*)-thiones. Comptes Rendus Chimie. 17, 1057-1064. https://doi.org/10.1016/j.crci.2013.12.006.

Rego, Y.F., Marcelo, P., Queiroz, T., Brito, O., Priscila, G., Vagner, C., Queiroz, T., Fátima, A., Macedo F., (2018). A review on the development of urease inhibitors as antimicrobial agents against pathogenic bacteria. J Adv Res. 13, 69–100. https://doi.10.1016/j.jare.2018.05.003.

Shamim, S., Khan, K.M., Salar, U., Ali, F., Lodhi, M.A., Taha, M., Khan, F.A., Ashraf, S., Ul-Haq, Z., Ali, M., Perveen, S., (2018). 5-Acetyl-6-methyl-4-aryl-3,4-dihydropyrimidin-2(1H)-ones: As potent urease inhibitors; synthesis, in vitro screening, and molecular modeling study. Bioorg. Chem. 76, 37–52. https://doi.org/10.1016/j.bioorg.2017.10.021.

Stingl, K., Altendorf, K., Bakker, E.P., (2002). Acid survival of Helicobacter pylori: how does urease activity trigger cytoplasmic pH homeostasis? Trends Microbiol.10, 70-74. https://10.1016/s0966-842x(01)02287-9.

Taha, M., Ismail, N.H., Imran, S., Wadood, A., Rahim, F., Riaz, M., (2015). Synthesis of potent urease inhibitors based on disulfide scaffold and their molecular docking studies. J. Bioorg. Med. Chem. 23, 7211–7218. https://doi.10.1016/j.bmc.2015.10.017.

Weatherburn, M., (1967). Phenol-hypochlorite reaction for determination of ammonia, Anal. Chem. 39, 971–974. https://doi.org/10.1021/ac60252a045.

Weber, M., Jones, M.J., Ulrich, J., (2008). Optimization of isolation and purification of the jack bean enzyme urease by extraction and subsequent crystallization. J. Food. Bioprod. Proc. 86, 43–52. https://doi.10.1016/j.fbp.2007.10.005.

مثبطات اليورياز الفعالة: التصميم والتشييد والإرتباط الجزيئي وتقييم الخواص الحركية لهجين داي هيدروبيرميدين فيثاليميد

أحمد أبو الفتوح السيد مراد[١،*]، مي أبوالفتوح السيد مراد[٢]

[١] قسم الأدوية والسموم- كلية الصيدلة- جامعة بورسعيد

[٢] قسم الكيمياء الطبية- كلية الصيدلة- جامعة بورسعيد

***البريد الإلكتروني للباحث الرئيسي:** ahmed.mourad@yahoo.com

الملخص:

حظي تثبيط عمل إنزيم اليورياز باهتمام كبير للتغلب على العديد من أمراض الجهاز الهضمي والكلى مثل القرحة المعدية وحصوات الجهاز البولي وكذلك التهاب حوض الكلى. تهدف الدراسة الحالية إلى تشييد هجائن ديهيدروبيريميدين فثاليميد الجديدة وتقييم نشاطها المثبط لعمل إنزيم اليورياز. كما تم اختبار مدى سمية المركبات المحضرة. بالإضافة إلى ذلك ، تم تقييم الخواص الحركية الدوائية لجميع الهجائن المحضرة. وأشارت النتائج إلى أنه من بين الهجائن المُحضرة ، حققت المركبات ١٠ج ، ١٠ هـ ، ١٠ س ، ١٠ ط ، ١٠ جي نشاطًا مثبطًا لليورياز بشكل أقوى حيث تراوحت IC_{50} من ١٢.٦ ± ٠.١ إلى ٢٠.١ ± ١.٣ ميكرومول ، مقارنةً بمثبط اليورياز القياسي ، الثيوريا مع IC_{50} من ٢١.٠ ± ٠.١ ميكرومول. كما كشفت دراسة الالتحام الجزيئي أن أكثر المركبات نشاطًا تلتحم جيدًا بالمواقع النشطة لإنزيم اليورياز وذلك تمشيا مع النتائج التي تم قياسها. وخلصت الدراسة إلى أن الطبيعة الإلكترونية ، وقابلية المركبات للذوبان في الدهون أو الماء، والعامل الفراغي للبدائل أثرت بشكل ملحوظ على النشاط المثبط لليورياز. كما أظهرت دراسة الخواص الحركية إلى أن المركبات المحضرة تتمتع بإمتصاص جيد من خلال الفم ولها نافذية ضعيفة للوصول إلى الجهاز العصبي المركزي. وتعتبر المركبات المشيدة آمنة كما هو موضح في اختبار السمية الخلوية.

الكلمات المفتاحية: مثبطات اليوريا ، ديهيدروبيريميدين ، فثاليميد ، السمية الخلوية ، القرحة المعدية ، التهاب حوض الكلي، جرثومة المعدة.